Bull. Mater. Sci., Vol. 40, No. 4, August 2017, pp. 841–857
DOI 10.1007/s12034-017-1425-x

Study of gamma radiation shielding properties of $ZnO-TeO_2$ glasses

SHAMS A M ISSA[1,2,*], M I SAYYED[2] and MURAT KURUDIREK[3]

[1]Physics Department, Faculty of Science, Al-Azhar University, Cairo, Egypt
[2]Physics Department, Faculty of Science, University of Tabuk, Tabuk, Saudi Arabia
[3]Department of Physics, Faculty of Science, Ataturk University, 25240 Erzurum, Turkey
*Author for correspondence (shams_issa@yahoo.com)

MS received 28 May 2016; accepted 24 October 2016; published online 25 July 2017

Abstract. Mass attenuation coefficient (μ_m), half value layer (HVL) and mean free path (MFP) for xZnO$-(100-x)$ TeO_2, where $x = 10$, 15, 20, 25, 30, 35 and 40 mol%, have been measured for 0.662, 1.173 and 1.33 MeV photons emitted from ^{137}Cs and ^{60}Co using a 3 × 3 inch NaI(Tl) detector. Some relevant parameters such as effective atomic numbers (Z_{eff}) and electron densities (N_{el}) of glass samples have been also calculated in the photon energy range of 0.015–15 MeV. Moreover, gamma-ray energy absorption buildup factor (EABF) and exposure buildup factor (EBF) were estimated using a five-parameter Geometric Progression (GP) fitting approximation, for penetration depths up to 40 MFP and in the energy range 0.015–15 MeV. The measured mass attenuation coefficients were found to agree satisfactorily with the theoretical values obtained through WinXcom. Effective atomic numbers (Z_{eff}) and electron densities (N_{el}) were found to be the highest for 40ZnO−60TeO_2 glass in the energy range 0.04–0.2 MeV. The 10ZnO−90TeO_2 glass sample has lower values of gamma-ray EBFs in the intermediate energy region. The reported new data on radiation shielding characteristics of zinc tellurite glasses should be beneficial from the point of proper gamma shield designs when intended to be used as radiation shields.

Keywords. Mass attenuation coefficient; effective atomic number; electron density; exposure buildup factors; tellurite glass.

1. Introduction

High-energy gamma rays are a type of electromagnetic radiation taking place in environment via radioisotopes or other radiation sources and they can be transferred anywhere so fast and cover distances of kilometers within seconds. Gamma-ray isotopes have been used excessively in many fields such as industry, agriculture and medicine. It is very important to develop effective radiation shielding materials by the formation of a mixture of materials as a shield against nuclear radiation [1–3]. The materials having high-atomic-number constituents such as tellurites ($Z = 52$) are the choice of radiation shields due to high attenuation of X-ray, gamma ray and fast neutrons [4]. The preparation and modification of transparent glass are essential for the development of a proper radiation shield. Tellurites transmit wavelength range from 0.5 to 6 μm, display mechanical and thermal stability and are not photosensitive [5–9]. The addition of ZnO to tellurite increases the glass formation and thermal stability [10,11].

Gamma radiation shielding properties of different compounds were evaluated using parameters such as mass attenuation coefficient (μ_m), half value layer (HVL), effective atomic number (Z_{eff}), electron density (N_{el}) and buildup factors (BFs) [12]. The exposure buildup factor (EBF) stands for exposure in air after penetration through the absorber or shielding material. Since a primary assessment in radiation protection is the exposure field before and after use of a radiation shield, EBFs are of more general use with appropriate adjustments of the air exposure to obtain absorbed dose [13]. The buildup factor values have been computed by various codes such as Geometric Progression (GP) method [14], iterative method [15], invariant embedding method [16,17] and Monte Carlo method [18]. American National Standards ANSI/ANS 6.4.3 [19] used GP fitting method and provided buildup factor data for 23 elements, water, air and concrete at 25 standard energies in the energy range 0.015–15 MeV with suitable interval up to the penetration depth of 40 mean free paths (MFPs).

While several studies have been made in order to investigate the radiation attenuation in different glass samples [20–25], the radiation shielding characteristics of the selected zinc tellurite glasses have not been investigated yet. This prompted us to carry out this work. In the present work, the mass attenuation coefficients have been measured for tellurite glasses at photon energies 0.662, 1.173 and 1.33 MeV. Effective atomic numbers (Z_{eff}) and electron densities (N_{el}) of glass samples have been calculated in the energy range 0.015–15 MeV. Gamma-ray energy absorption buildup factor (EABF) and

EBF of glass systems were computed for penetration depths up to 40 MFP and in the energy range 0.015–15 MeV.

2. Experimental

2.1 *Sample preparation*

A glass system of composite xZnO–$(100-x)$$TeO_3$ where $x = 10, 15, 20, 25, 30, 35$ and 40 mol% was prepared by the rapid melt quenching technique using chemicals TeO_3 and ZnO (99.99%). Reactants taken in exact mole ratios were mixed thoroughly in an agate mortar. The mixtures were initially heated in a ceramic crucible kept in an electrical muffle furnace at 1073 K for 60 min and the melt was swirled frequently to ensure proper mixing and homogeneity. The melt was then quenched to room temperature. The obtained samples were annealed by transferring them into another electrical furnace at a temperature of 623 K for 4 h and slowly cooled to room temperature to minimize cracking and thermal stresses of the glasses [26–28]. The samples were prepared with different thicknesses (0.5–1.3 cm). The relative error in the thickness was found to be ±0.002 cm. The densities of prepared glassy samples were determined by a simple Archimedes method using an immersing liquid such as acetone. The chemical composition of glass samples, densities, molar volume and thickness are listed in table 1.

2.2 *Measurements*

Mass attenuation coefficient measurements were performed using a gamma-ray spectrometer, employing a scintillation detector (3 × 3 inch) (figure 1). Its hermetically sealed assembly includes a high-resolution NaI(Tl) crystal, photomultiplier tube, an internal magnetic/light shield, aluminium housing and a 14-pin connector coupled to a PC-MCA Canberra Accuspes. It has the following specifications: (1) 7.5% resolution specified at the 662 keV peak of ^{137}Cs, (2) aluminium window 0.5 mm thick and density 147 mg cm^{-2}, (3) reflector oxide 1.6 mm thick and density 88 mg cm^{-2}, (4) magnetic/light shield—Co-NETIC-lined steel and (5) operating voltage positive 902 V (DC). A dedicated software program, Genie 2000 from Canberra, was used to carry out the on-line analysis of each measured gamma-ray spectrum. The detection array was energy calibrated using ^{60}Co (1173.2 and 1332.5 keV), ^{133}Ba (356.1 keV) and ^{137}Cs (661.9 keV).

The experimental mass attenuation coefficients (μ_m) of glass samples have been measured using the well-known Beer–Lambert equation:

$$\mu_m = \frac{\ln(I_0/I)}{\rho t}, \tag{1}$$

where I_0 and I are the incident and transmitted intensities, ρ is density of the material (g cm^{-3}) and t is the thickness

Table 1. Chemical composition, density, molar volume (M_v) and thickness of glass samples.

Sample no.	Composition (mole fraction) ZnO	TeO_2	Density ρ (g cm^{-3})	M_v (cm^3 mol^{-1})	Thickness* (cm)
1	10	90	5.048 ± 0.050	30.067	0.523
2	15	85	5.063 ± 0.051	29.205	0.633
3	20	80	5.101 ± 0.051	28.221	0.752
4	25	75	5.111 ± 0.051	27.401	0.834
5	30	70	5.149 ± 0.051	26.439	0.912
6	35	65	5.161 ± 0.052	25.620	1.254
7	40	60	5.181 ± 0.052	24.766	1.321

*The relative error in thickness was found to be ±0.002 cm.

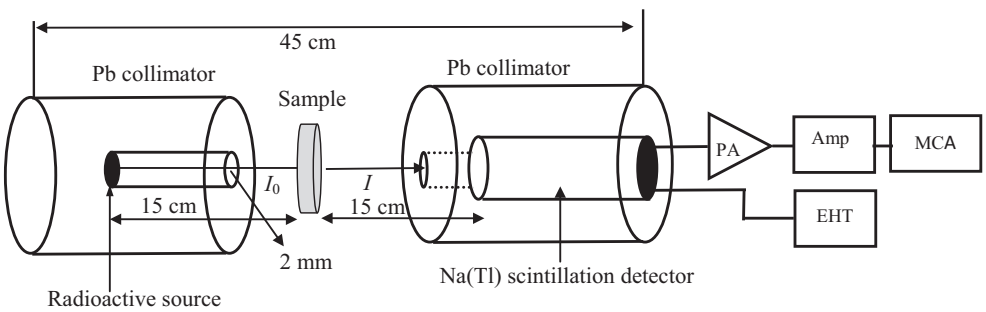

Figure 1. Narrow-beam experiment geometry.

Table 2. Theoretical $(\mu_m)_{Xcom}$ and experimental $(\mu_m)_{exp}$ mass attenuation coefficient of glass systems.

	$\mu_m \times 10^{-2}$ (cm^2 g^{-1})					
	0.662 MeV		1.173 MeV		1.33 MeV	
Sample no.	WinXcom	Exp.	WinXcom	Exp.	WinXcom	Exp.
1	7.272	7.138 ± 0.134	5.322	5.216 ± 0.106	4.971	4.872 ± 0.099
2	7.274	7.156 ± 0.118	5.335	5.227 ± 0.108	4.984	4.884 ± 0.100
3	7.275	7.149 ± 0.126	5.347	5.239 ± 0.108	4.998	4.898 ± 0.100
4	7.276	7.127 ± 0.149	5.360	5.258 ± 0.102	5.011	4.911 ± 0.100
5	7.278	7.135 ± 0.143	5.373	5.276 ± 0.097	5.024	4.924 ± 0.100
6	7.279	7.142 ± 0.137	5.386	5.277 ± 0.109	5.037	4.936 ± 0.101
7	7.28	7.139 ± 0.141	5.399	5.305 ± 0.094	5.050	4.949 ± 0.101

Table 3. Experimental half value layer (HVL) and mean free path (MFP) of glass systems.

	HVL (cm)			MFP (cm)		
Sample no.	0.662 MeV	1.173 MeV	1.330 MeV	0.662 MeV	1.173 MeV	1.330 MeV
1	1.893	2.590	2.773	2.73	3.74	4.00
2	1.885	2.572	2.754	2.72	3.71	3.97
3	1.870	2.546	2.724	2.70	3.67	3.93
4	1.866	2.534	2.711	2.69	3.66	3.91
5	1.852	2.509	2.684	2.67	3.62	3.87
6	1.847	2.497	2.670	2.66	3.60	3.85
7	1.839	2.480	2.651	2.65	3.58	3.83

of the absorber (cm). The glass samples were irradiated by 0.662, 1.173 and 1.33 MeV photons from 5 μCi ^{137}Cs and ^{60}Co radioactive sources. The measurements were taken for 4 h and were repeated 5 times for each sample.

3. Calculations

3.1 *Effective atomic number and electron density*

Total photon interaction cross-section (σ_t) of the glasses is determined with the help of the mass attenuation coefficient (μ_m) through the following equation:

$$\sigma_t = \frac{M\mu_m}{N_A}, \tag{2}$$

where $M = \sum_i A_i n_i$ is the molecular weight of the sample, A_i is the atomic weight of the ith element, n_i the number of formula units of a molecule and N_A is Avogadro's number.

Effective atomic cross-section σ_a is calculated using the following equation:

$$\sigma_a = \frac{\sigma_t}{\sum_i n_i}. \tag{3}$$

Total electronic cross-section σ_e is calculated using the relation

$$\sigma_e = \frac{1}{N_A}\sum_i \frac{f_i A_i}{Z_i}(\mu_m)_{i,} \tag{4}$$

where f_i denotes the fractional abundance of the element i and Z_i the atomic number of constituent element.

The effective atomic number (Z_{eff}) is related to σ_a and σ_e through the following equation:

$$Z_{eff} = \frac{\sigma_a}{\sigma_e}. \tag{5}$$

Electron density (number of electrons per unit mass, N_{el}) of the sample can be calculated from the relation

$$N_{el} = \frac{Z_{eff}N_A}{M}\sum_i n_i \left(\text{electron g}^{-1}\right). \tag{6}$$

3.2 *Buildup factors*

The logarithmic interpolation method from the equivalent atomic number (Z_{eq}) was used to calculate EBF values and the GP fitting parameters of the tellurite glass samples. Computations are illustrated step by step as follows:

a. calculation of equivalent atomic number (Z_{eq});
b. calculation of GP fitting parameters and
c. calculation of EBFs.

A single element has atomic number Z; the zinc tellurite glasses have an equivalent atomic number (Z_{eq}) that describes the properties of glass systems. Because the gamma-ray partial interaction processes with material depend on the energy, Z_{eq} is an energy-dependent parameter. Using the winXCom program [29,30], the total mass attenuation coefficient of selected ZnO–TeO_2 glasses and Compton partial mass attenuation coefficient for elements from $Z = 4$ to 50 were obtained in the energy range 0.015–15 MeV. The equivalent atomic number has been calculated by matching the ratio of Compton partial mass attenuation coefficient to the total mass attenuation coefficient of selected glass systems with identical ratio of a single element of the same energy. The following formula was used to interpolate the Z_{eq} [31]:

$$Z_{eq} = \frac{Z_1\,(\log R_2 - \log R) + Z_2\,(\log R - \log R_1)}{\log R_2 - \log R_1}, \tag{7}$$

where Z_1 and Z_2 are the atomic numbers of elements corresponding to the ratios R_1 and R_2, respectively, and R is the ratio of the glass samples at a specific energy. For example the ratio $(\mu/\rho)_{\text{Compton}} / (\mu/\rho)_{\text{total}}$ of $10\text{ZnO} - 90\text{TeO}_2$ at the energy of 0.3 MeV is 0.635, which lies between $R_1 = (\mu/\rho)_{\text{Compton}}/(\mu/\rho)_{\text{total}} = 0.628$ of $Z_1 = 46$ and $R_2 = (\mu/\rho)_{\text{Compton}}/(\mu/\rho)_{\text{total}} = 0.645$ of $Z = 47$; using equation (7), $Z_{eq} = 46.42$ is calculated.

GP fitting parameters are calculated in a same way of logarithmic interpolation method for Z_{eq}.

The GP fitting parameters for the elements were taken from the report by American Nuclear Society [19]. The GP fitting parameters for the glass samples were logarithmically interpolated using the same formula as follows [31]:

$$C = \frac{C_1\left(\log Z_2 - \log Z_{eq}\right) + C_2\left(\log Z_{eq} - \log Z_1\right)}{\log Z_2 - \log Z_1}, \tag{8}$$

where C_1 and C_2 are the values of the GP fitting parameters corresponding to the atomic numbers Z_1 and Z_2, respectively, at a given energy.

The GP fitting parameters were used to calculate the EBFs of glasses as follows [32]:

$$B\,(E, X) = 1 + \frac{b-1}{K-1}\left(K^x - 1\right) \qquad \text{for } K \neq 1, \tag{9}$$

$$B\,(K, X) = 1 + (b-1)\,x \qquad \text{for } K = 1, \tag{10}$$

where

$$K\,(E, x) = cx^a + d\frac{\tanh\left((x/X_k) - 2\right) - \tanh(-2)}{1 - \tanh(-2)} \quad \text{for } x \leq 40 \text{ MFP}, \tag{11}$$

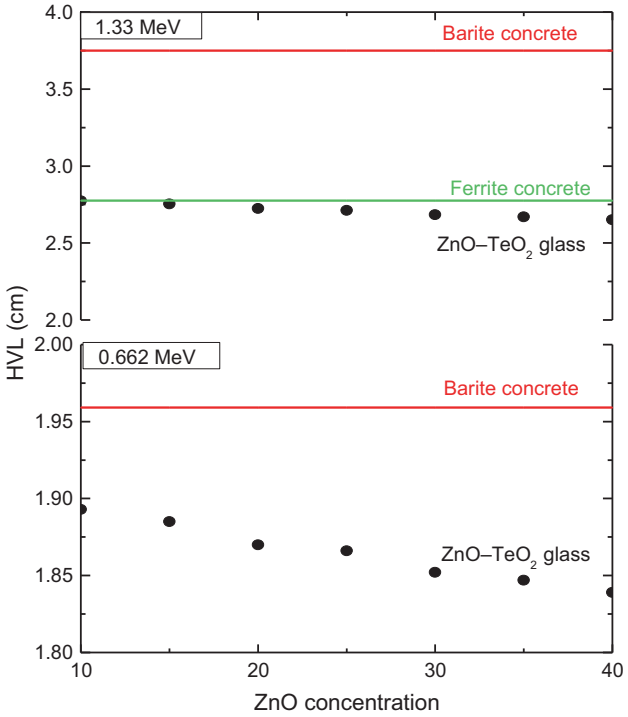

Figure 2. Variation of half value layer as a function of ZnO oxide at 0.662 and 1.33 MeV photon energy in the (filled circle) ZnO–TeO_2 glass systems. Theoretical values at the same energies for (red line) barite concrete and (green line) ferrite concrete.

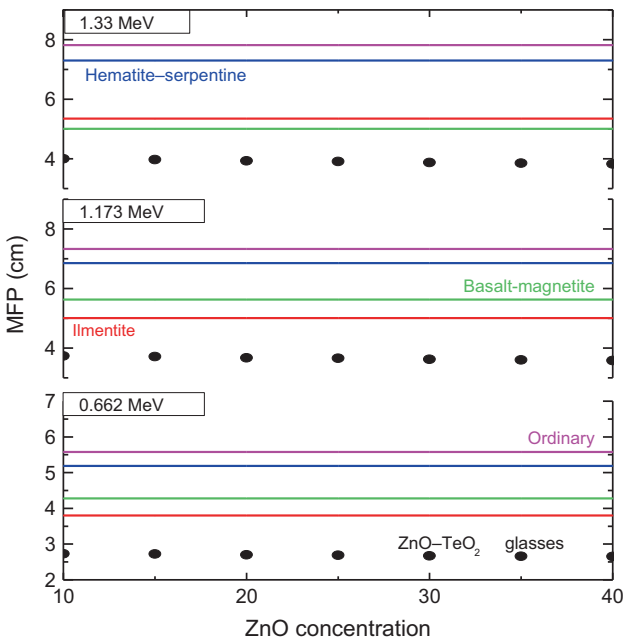

Figure 3. Variation of mean free path as a function of ZnO concentration at 0.662, 1.173 and 1.33 MeV photon energy in the (filled circle) ZnO–TeO_2 glass systems. Theoretical values at the same energies for (pink line) ordinary concrete, (blue line) hematite-serpentine, (green line) basalt-magnetite and (red line) ilmentite.

Table 4. Effective atomic number (Z_{eff}) and electron density ($N_{el} \times 10^{23}$) of glass samples.

	10ZnO		15ZnO		20ZnO		25ZnO		30ZnO		35ZnO		40ZnO	
Energy (MeV)	Z_{eff}	N_{el}	Z_{eff}	N_{el}	Z_{eff}	N_{el}	Z_{eff}	N_{el}	Z_{eff}	N_{el}	Z_{eff}	N_{el}	Z_{eff}	N_{el}
0.015	33.087	4.134	34.081	4.258	35.074	4.382	36.068	4.507	37.062	4.631	38.056	4.755	39.050	4.879
0.02	32.977	4.120	33.986	4.246	34.995	4.372	36.003	4.498	37.012	4.624	38.021	4.750	39.029	4.876
0.03	32.859	4.106	33.838	4.228	34.816	4.350	35.795	4.472	36.773	4.595	37.752	4.717	38.730	4.839
0.04	57.927	7.238	55.608	6.948	53.289	6.658	50.971	6.368	48.652	6.079	46.333	5.789	44.014	5.499
0.05	57.667	7.205	55.331	6.913	52.995	6.621	50.659	6.329	48.322	6.038	45.986	5.746	43.650	5.454
0.06	56.989	7.120	54.672	6.831	52.355	6.541	50.039	6.252	47.722	5.963	45.406	5.673	43.089	5.384
0.08	54.585	6.820	52.395	6.546	50.205	6.273	48.016	5.999	45.826	5.726	43.637	5.452	41.447	5.179
0.1	51.195	6.397	49.214	6.149	47.233	5.901	45.252	5.654	43.270	5.406	41.289	5.159	39.308	4.911
0.15	41.771	5.219	40.408	5.049	39.046	4.879	37.683	4.708	36.320	4.538	34.957	4.368	33.594	4.197
0.2	34.468	4.307	33.601	4.198	32.734	4.090	31.868	3.982	31.001	3.873	30.134	3.765	29.268	3.657
0.3	27.043	3.379	26.690	3.335	26.336	3.291	25.983	3.246	25.629	3.202	25.276	3.158	24.923	3.114
0.4	24.179	3.021	24.026	3.002	23.873	2.983	23.720	2.964	23.567	2.945	23.414	2.925	23.261	2.906
0.5	22.891	2.860	22.829	2.852	22.767	2.845	22.705	2.837	22.643	2.829	22.581	2.821	22.520	2.814
0.6	22.229	2.777	22.214	2.776	22.200	2.774	22.185	2.772	22.170	2.770	22.156	2.768	22.141	2.766
0.8	21.596	2.698	21.626	2.702	21.657	2.706	21.688	2.710	21.718	2.714	21.749	2.717	21.779	2.721
1	21.310	2.663	21.361	2.669	21.412	2.675	21.463	2.682	21.514	2.688	21.565	2.694	21.616	2.701
1.5	21.185	2.647	21.249	2.655	21.312	2.663	21.376	2.671	21.439	2.679	21.503	2.687	21.566	2.695
2	21.505	2.687	21.557	2.693	21.608	2.700	21.659	2.706	21.710	2.713	21.762	2.719	21.813	2.725
3	22.548	2.817	22.557	2.818	22.567	2.820	22.576	2.821	22.585	2.822	22.595	2.823	22.604	2.824
4	23.681	2.959	23.645	2.954	23.609	2.950	23.573	2.945	23.537	2.941	23.501	2.936	23.465	2.932
5	25.720	3.214	25.606	3.199	25.491	3.185	25.377	3.171	25.262	3.156	25.148	3.142	25.033	3.128
6	27.353	3.418	27.177	3.396	27.001	3.374	26.825	3.352	26.649	3.330	26.473	3.308	26.297	3.286
8	28.649	3.579	28.423	3.551	28.198	3.523	27.973	3.495	27.747	3.467	27.522	3.439	27.297	3.411
10	30.887	3.859	30.573	3.820	30.259	3.781	29.945	3.742	29.632	3.702	29.318	3.663	29.004	3.624
15	33.087	4.134	34.081	4.258	35.074	4.382	36.068	4.507	37.062	4.631	38.056	4.755	39.050	4.879

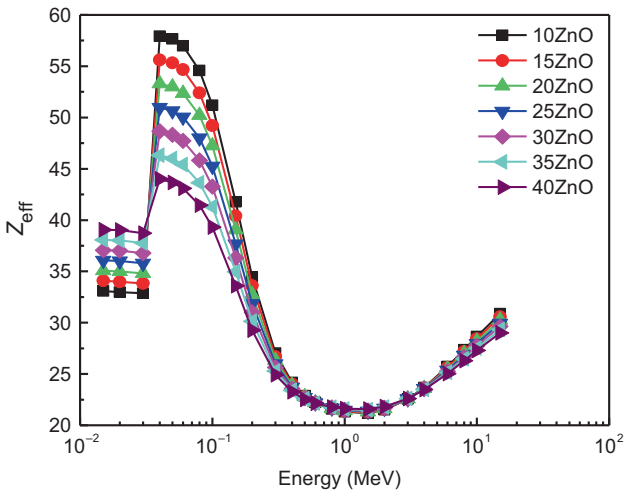

Figure 4. The variation of Z_{eff} with photon energy of glass samples.

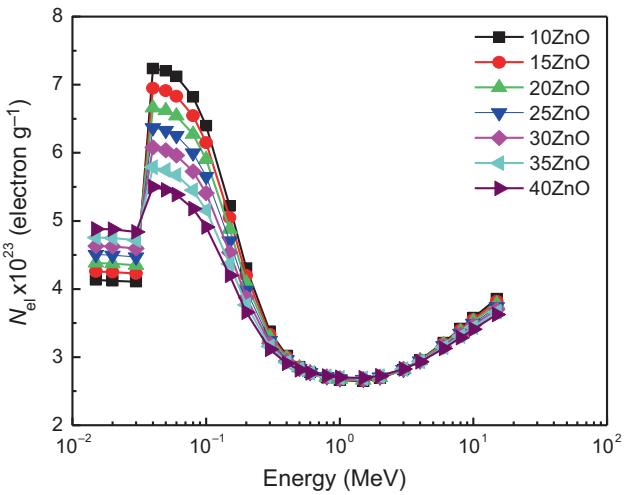

Figure 5. The variation of N_{el} with photon energy of glass samples.

where E is the incident photon energy and x is the penetration depth in MFP; $a-d$ and X_k are the GP fitting parameters. The variation of the parameter K with penetration depth represents the photon dose multiplication and a change in the shape of the spectrum.

4. Result and discussion

The density (ρ) and the molar volume (M_v) of the investigated glasses are listed in table 1. It is observed that the density of glass increases from 5.048 to 5.181 (g m^{-3}) with the

Table 5. Equivalent atomic number (Z_{eq}) and GP exposure (EBF) and energy absorption (EABF) buildup factor coefficients for $10ZnO–90TeO_2$ glass sample.

		EBF					EABF				
Energy (MeV)	Z_{eq}	b	c	a	X_k	d	b	c	a	X_k	d
0.015	24.78	1.005	1.385	−0.449	5.861	0.312	1.005	1.383	−0.447	6.353	0.308
0.02	24.89	1.013	0.182	0.547	11.307	−0.528	1.011	0.277	0.307	17.061	−0.275
0.03	25.12	1.032	0.374	0.195	26.998	−0.291	1.031	0.324	0.250	18.081	−0.185
0.04	44.48	3.820	0.618	0.091	24.341	−0.063	1.545	0.630	0.101	13.253	−0.039
0.05	44.90	3.254	0.212	−0.088	13.814	−0.056	1.481	0.221	−0.084	11.511	−0.016
0.06	45.19	2.634	0.101	0.628	12.258	−0.109	1.428	0.121	0.430	17.541	−0.088
0.08	45.57	1.730	0.026	0.788	14.892	−0.208	1.344	0.059	0.648	14.134	−0.228
0.1	45.81	1.276	0.179	0.488	13.770	−0.238	1.265	0.161	0.493	13.601	−0.263
0.15	46.16	1.229	0.401	0.231	14.165	−0.126	1.442	0.245	0.363	13.970	−0.201
0.2	46.35	1.353	0.506	0.172	14.477	−0.095	1.909	0.293	0.323	13.968	−0.194
0.3	46.58	1.480	0.682	0.095	14.336	−0.047	2.107	0.498	0.186	13.917	−0.109
0.4	46.70	1.601	0.828	0.054	14.156	−0.039	2.424	0.639	0.134	13.886	−0.100
0.5	46.78	1.672	0.912	0.033	14.163	−0.031	2.491	0.753	0.092	13.881	−0.077
0.6	46.84	1.702	0.968	0.017	13.990	−0.022	2.492	0.819	0.069	13.741	−0.064
0.8	46.88	1.728	1.026	0.002	14.064	−0.016	2.406	0.902	0.043	13.641	−0.049
1	46.90	1.721	1.052	−0.004	13.430	−0.014	2.299	0.946	0.029	13.518	−0.041
1.5	46.12	1.595	1.140	−0.025	10.981	−0.002	1.928	1.062	−0.003	13.572	−0.020
2	44.16	1.588	1.122	−0.020	12.758	−0.006	1.850	1.032	0.007	13.084	−0.028
3	41.70	1.558	1.065	0.000	12.828	−0.028	1.719	0.958	0.033	13.192	−0.056
4	40.76	1.508	1.023	0.015	13.324	−0.041	1.595	0.915	0.050	13.565	−0.071
5	40.25	1.514	0.950	0.042	13.552	−0.066	1.556	0.851	0.096	13.823	−0.095
6	39.90	1.487	0.931	0.052	13.738	−0.074	1.496	0.835	0.086	14.041	−0.103
8	39.49	1.501	0.892	0.073	14.042	−0.091	1.448	0.820	0.099	14.250	−0.112
10	39.28	1.464	0.964	0.056	14.156	−0.075	1.379	0.892	0.079	14.346	−0.093
15	39.18	1.501	1.090	0.038	14.220	−0.061	1.357	1.004	0.062	14.379	−0.081

Table 6. Equivalent atomic number (Z_{eq}) and GP exposure (EBF) and energy absorption (EABF) buildup factor coefficients for $15ZnO–85TeO_2$ glass sample.

		EBF					EABF				
Energy (MeV)	Z_{eq}	b	c	a	X_k	d	b	c	a	X_k	d
0.015	24.95	1.004	1.409	−0.463	5.826	0.317	1.004	1.407	−0.461	6.250	0.308
0.02	25.06	1.013	0.174	0.558	11.319	−0.541	1.011	0.274	0.309	17.238	−0.275
0.03	25.28	1.031	0.374	0.194	27.445	−0.296	1.030	0.323	0.250	18.233	−0.185
0.04	43.69	3.858	0.526	0.090	24.039	−0.053	1.528	0.534	0.103	13.243	−0.039
0.05	44.13	3.216	0.167	−0.147	13.334	−0.027	1.456	0.177	−0.102	10.680	−0.016
0.06	44.44	2.582	0.078	0.737	13.472	−0.118	1.405	0.099	0.515	16.934	−0.088
0.08	44.82	1.716	0.027	0.783	14.791	−0.217	1.335	0.063	0.633	14.115	−0.228
0.1	45.06	1.254	0.202	0.451	13.766	−0.223	1.252	0.179	0.462	13.637	−0.263
0.15	45.44	1.231	0.416	0.221	14.208	−0.120	1.443	0.258	0.351	13.992	−0.201
0.2	45.64	1.372	0.507	0.172	14.447	−0.096	1.967	0.296	0.322	13.978	−0.194
0.3	45.88	1.496	0.689	0.093	14.358	−0.047	2.148	0.507	0.182	13.938	−0.109
0.4	46.02	1.617	0.837	0.052	14.159	−0.038	2.459	0.649	0.130	13.889	−0.100
0.5	46.09	1.686	0.921	0.030	14.186	−0.030	2.519	0.764	0.088	13.884	−0.077
0.6	46.14	1.715	0.976	0.015	13.983	−0.022	2.514	0.829	0.066	13.744	−0.064
0.8	46.19	1.738	1.033	0.001	14.058	−0.016	2.419	0.911	0.040	13.644	−0.049
1	46.22	1.730	1.057	−0.005	13.430	−0.014	2.309	0.953	0.027	13.523	−0.041
1.5	45.39	1.600	1.144	−0.026	10.323	−0.002	1.930	1.067	−0.004	13.555	−0.020
2	43.32	1.593	1.124	−0.020	12.705	−0.006	1.850	1.038	0.005	13.079	−0.028
3	40.83	1.562	1.065	0.000	12.792	−0.027	1.716	0.963	0.031	13.138	−0.056
4	39.87	1.511	1.023	0.015	13.298	−0.040	1.592	0.921	0.048	13.599	−0.071
5	39.36	1.512	0.954	0.041	13.532	−0.063	1.549	0.861	0.103	13.845	−0.095
6	39.03	1.483	0.936	0.050	13.703	−0.071	1.488	0.845	0.082	14.059	−0.103
8	38.63	1.491	0.897	0.071	14.003	−0.089	1.437	0.830	0.094	14.236	−0.112
10	38.42	1.451	0.964	0.055	14.138	−0.073	1.368	0.897	0.076	14.345	−0.093
15	38.32	1.478	1.081	0.039	14.239	−0.061	1.341	1.000	0.062	14.411	−0.081

Table 7. Equivalent atomic number (Z_{eq}) and GP exposure (EBF) and energy absorption (EABF) buildup factor coefficients for $20ZnO–80TeO_2$ glass sample.

		EBF					EABF				
Energy (MeV)	Z_{eq}	b	c	a	X_k	d	b	c	a	X_k	d
0.015	25.11	1.004	1.432	−0.477	5.791	0.323	1.004	1.431	−0.476	6.149	0.320
0.02	25.22	1.012	0.166	0.569	11.332	−0.555	1.011	0.271	0.311	17.412	−0.281
0.03	25.44	1.030	0.374	0.193	27.873	−0.301	1.029	0.322	0.251	18.379	−0.188
0.04	42.90	3.896	0.431	0.089	23.728	−0.043	1.510	0.434	0.105	13.232	−0.043
0.05	43.34	3.177	0.120	−0.209	12.835	0.003	1.429	0.132	−0.121	9.814	0.057
0.06	43.66	2.528	0.055	0.851	14.732	−0.127	1.381	0.075	0.604	16.304	−0.136
0.08	44.05	1.701	0.029	0.779	14.687	−0.228	1.325	0.068	0.617	14.095	−0.228
0.1	44.31	1.231	0.225	0.412	13.762	−0.207	1.238	0.196	0.430	13.673	−0.227
0.15	44.70	1.233	0.431	0.211	14.252	−0.113	1.444	0.271	0.337	14.014	−0.187
0.2	44.91	1.392	0.509	0.172	14.417	−0.096	2.028	0.298	0.321	13.988	−0.196
0.3	45.17	1.512	0.697	0.091	14.382	−0.046	2.191	0.516	0.178	13.960	−0.105
0.4	45.31	1.633	0.846	0.050	14.163	−0.037	2.496	0.660	0.126	13.893	−0.096
0.5	45.39	1.700	0.930	0.028	14.210	−0.029	2.548	0.775	0.085	13.887	−0.074
0.6	45.44	1.728	0.984	0.013	13.976	−0.021	2.537	0.839	0.063	13.746	−0.061
0.8	45.49	1.749	1.039	−0.001	14.052	−0.015	2.433	0.920	0.038	13.646	−0.047
1	45.52	1.738	1.063	−0.007	13.430	−0.013	2.318	0.961	0.025	13.527	−0.038
1.5	44.64	1.605	1.147	−0.027	9.640	−0.001	1.933	1.073	−0.006	13.537	−0.018
2	42.47	1.598	1.126	−0.021	12.651	−0.006	1.850	1.044	0.003	13.073	−0.025
3	39.95	1.565	1.064	−0.001	12.755	−0.026	1.714	0.967	0.030	13.083	−0.052
4	39.00	1.513	1.023	0.015	13.272	−0.039	1.588	0.928	0.045	13.632	−0.066
5	38.50	1.510	0.958	0.039	13.512	−0.061	1.542	0.871	0.109	13.867	−0.087
6	38.17	1.479	0.940	0.048	13.668	−0.069	1.480	0.856	0.077	14.077	−0.094
8	37.77	1.480	0.901	0.068	13.964	−0.086	1.425	0.840	0.090	14.221	−0.103
10	37.57	1.438	0.964	0.054	14.120	−0.072	1.357	0.902	0.073	14.344	−0.087
15	37.47	1.455	1.072	0.040	14.259	−0.061	1.325	0.995	0.061	14.443	−0.078

Table 8. Equivalent atomic number (Z_{eq}) and GP exposure (EBF) and energy absorption (EABF) buildup factor coefficients for $25ZnO–75TeO_2$ glass sample.

		EBF					EABF				
Energy (MeV)	Z_{eq}	b	c	a	X_k	d	b	c	a	X_k	d
0.015	25.26	1.004	1.455	−0.491	5.757	0.328	1.004	1.454	−0.490	6.052	0.326
0.02	25.38	1.012	0.159	0.579	11.344	−0.567	1.011	0.268	0.312	17.579	−0.284
0.03	25.60	1.030	0.374	0.192	28.282	−0.305	1.029	0.321	0.251	18.519	−0.189
0.04	42.10	3.936	0.334	0.088	23.411	−0.033	1.491	0.333	0.107	13.221	−0.045
0.05	42.55	3.137	0.072	−0.272	12.322	0.034	1.402	0.085	−0.140	8.927	0.095
0.06	42.88	2.472	0.031	0.969	16.039	−0.137	1.356	0.051	0.695	15.651	−0.162
0.08	43.28	1.686	0.030	0.775	14.581	−0.238	1.316	0.073	0.601	14.074	−0.228
0.1	43.55	1.207	0.249	0.373	13.758	−0.190	1.224	0.215	0.397	13.711	−0.208
0.15	43.94	1.235	0.447	0.201	14.298	−0.107	1.445	0.285	0.324	14.038	−0.179
0.2	44.17	1.413	0.510	0.172	14.385	−0.097	2.091	0.300	0.320	13.998	−0.196
0.3	44.42	1.530	0.705	0.088	14.406	−0.045	2.235	0.526	0.174	13.983	−0.104
0.4	44.57	1.650	0.856	0.047	14.166	−0.036	2.535	0.672	0.122	13.896	−0.094
0.5	44.66	1.716	0.940	0.026	14.235	−0.028	2.579	0.786	0.081	13.889	−0.072
0.6	44.72	1.742	0.992	0.011	13.969	−0.021	2.560	0.850	0.060	13.749	−0.060
0.8	44.77	1.760	1.046	−0.002	14.046	−0.015	2.447	0.929	0.035	13.649	−0.045
1	44.80	1.747	1.069	−0.008	13.430	−0.012	2.328	0.969	0.023	13.531	−0.037
1.5	43.88	1.610	1.151	−0.028	8.928	0.000	1.935	1.078	−0.007	13.518	−0.017
2	41.61	1.603	1.127	−0.021	12.526	−0.005	1.850	1.050	0.001	12.980	−0.024
3	39.07	1.569	1.064	−0.001	12.717	−0.026	1.711	0.973	0.028	13.027	−0.049
4	38.13	1.516	1.023	0.014	13.245	−0.038	1.585	0.935	0.043	13.666	−0.063
5	37.64	1.507	0.962	0.037	13.492	−0.059	1.535	0.880	0.115	13.889	−0.083
6	37.31	1.475	0.945	0.045	13.631	−0.066	1.471	0.866	0.073	14.096	−0.089
8	36.93	1.469	0.907	0.065	13.924	−0.083	1.414	0.850	0.085	14.207	−0.098
10	36.73	1.425	0.964	0.053	14.101	−0.071	1.345	0.907	0.070	14.343	−0.084
15	36.64	1.432	1.063	0.041	14.278	−0.061	1.309	0.991	0.061	14.475	−0.077

Table 9. Equivalent atomic number (Z_{eq}) and GP exposure (EBF) and energy absorption (EABF) buildup factor coefficients for $30ZnO–70TeO_2$ glass sample.

		EBF					EABF				
Energy (MeV)	Z_{eq}	b	c	a	X_k	d	b	c	a	X_k	d
0.015	25.41	1.004	1.477	−0.504	5.725	0.333	1.004	1.476	−0.503	5.959	0.331
0.02	25.53	1.012	0.152	0.590	11.355	−0.579	1.010	0.266	0.314	17.735	−0.287
0.03	25.74	1.029	0.374	0.191	28.675	−0.310	1.028	0.320	0.251	18.651	−0.190
0.04	41.31	3.811	0.322	0.095	22.971	−0.035	1.469	0.323	0.111	23.319	−0.056
0.05	41.75	3.077	0.043	−0.308	11.975	0.053	1.378	0.057	−0.147	8.375	0.117
0.06	42.08	2.414	0.007	1.091	17.382	−0.147	1.330	0.026	0.789	14.979	−0.188
0.08	42.49	1.671	0.032	0.770	14.470	−0.249	1.306	0.078	0.584	14.053	−0.228
0.1	42.77	1.183	0.275	0.331	13.754	−0.173	1.209	0.234	0.362	13.751	−0.188
0.15	43.17	1.238	0.464	0.191	14.346	−0.100	1.446	0.299	0.309	14.062	−0.171
0.2	43.38	1.434	0.511	0.173	14.352	−0.098	2.158	0.303	0.319	14.010	−0.197
0.3	43.67	1.548	0.714	0.086	14.432	−0.044	2.281	0.536	0.169	14.006	−0.102
0.4	43.81	1.667	0.866	0.045	14.170	−0.036	2.577	0.684	0.117	13.900	−0.092
0.5	43.93	1.731	0.951	0.023	14.261	−0.027	2.611	0.798	0.077	13.892	−0.070
0.6	43.97	1.756	1.000	0.009	13.961	−0.020	2.585	0.861	0.056	13.752	−0.058
0.8	44.04	1.771	1.053	−0.004	14.039	−0.014	2.462	0.939	0.033	13.652	−0.044
1	44.02	1.757	1.075	−0.009	13.430	−0.012	2.339	0.978	0.020	13.537	−0.035
1.5	42.93	1.616	1.155	−0.029	8.171	0.000	1.938	1.086	−0.009	13.494	−0.016
2	40.79	1.609	1.127	−0.021	12.312	−0.005	1.849	1.053	0.000	12.787	−0.023
3	38.19	1.572	1.063	−0.001	12.678	−0.025	1.708	0.978	0.026	12.969	−0.047
4	37.27	1.518	1.023	0.014	13.218	−0.037	1.581	0.941	0.040	13.700	−0.060
5	36.44	1.505	0.966	0.035	13.472	−0.056	1.524	0.894	0.125	13.922	−0.077
6	36.44	1.471	0.949	0.043	13.595	−0.063	1.463	0.877	0.068	14.115	−0.085
8	36.12	1.458	0.912	0.063	13.884	−0.081	1.402	0.860	0.080	14.192	−0.094
10	35.89	1.411	0.964	0.052	14.082	−0.070	1.334	0.912	0.067	14.342	−0.081
15	35.80	1.408	1.054	0.042	14.298	−0.062	1.292	0.986	0.060	14.508	−0.076

Table 10. Equivalent atomic number (Z_{eq}) and GP exposure (EBF) and energy absorption (EABF) buildup factor coefficients for $35ZnO–65TeO_2$ glass sample.

		EBF					EABF				
Energy (MeV)	Z_{eq}	b	c	a	X_k	d	b	c	a	X_k	d
0.015	25.56	1.004	1.498	−0.516	5.694	0.338	1.004	1.497	−0.516	5.869	0.337
0.02	25.68	1.012	0.145	0.599	11.366	−0.591	1.010	0.263	0.316	17.891	−0.289
0.03	25.89	1.028	0.374	0.191	29.051	−0.314	1.027	0.319	0.252	18.782	−0.191
0.04	40.50	3.656	0.323	0.103	22.493	−0.038	1.617	0.394	0.097	22.135	−0.044
0.05	40.94	2.969	0.060	−0.279	12.024	0.042	1.467	0.128	−0.145	8.524	0.112
0.06	41.27	2.346	0.021	1.062	17.331	−0.147	1.317	0.038	0.773	14.206	−0.189
0.08	41.68	1.651	0.041	0.755	14.391	−0.253	1.299	0.087	0.566	14.047	−0.226
0.1	41.95	1.158	0.301	0.290	13.750	−0.155	1.195	0.254	0.327	13.809	−0.168
0.15	42.37	1.240	0.482	0.179	14.397	−0.093	1.447	0.314	0.294	14.088	−0.163
0.2	42.60	1.457	0.513	0.173	14.317	−0.099	2.226	0.305	0.319	14.021	−0.198
0.3	42.89	1.567	0.723	0.083	14.459	−0.044	2.330	0.547	0.165	14.031	−0.100
0.4	43.04	1.686	0.877	0.042	14.174	−0.035	2.619	0.697	0.112	13.904	−0.090
0.5	43.14	1.748	0.962	0.020	14.288	−0.026	2.645	0.811	0.073	13.895	−0.068
0.6	43.21	1.771	1.010	0.007	13.953	−0.019	2.610	0.873	0.053	13.755	−0.056
0.8	43.27	1.783	1.060	−0.005	14.032	−0.014	2.477	0.949	0.030	13.655	−0.042
1	43.29	1.767	1.081	−0.011	13.430	−0.011	2.350	0.986	0.018	13.541	−0.034
1.5	42.26	1.622	1.160	−0.030	7.385	0.001	1.940	1.091	−0.010	13.477	−0.015
2	39.85	1.614	1.126	−0.021	12.091	−0.005	1.848	1.057	−0.001	12.561	−0.022
3	37.31	1.576	1.063	−0.001	12.638	−0.024	1.705	0.983	0.023	12.909	−0.044
4	36.40	1.521	1.023	0.013	13.190	−0.036	1.578	0.949	0.037	13.736	−0.057
5	35.91	1.502	0.970	0.033	13.450	−0.054	1.520	0.901	0.129	13.936	−0.075
6	35.62	1.466	0.954	0.041	13.557	−0.061	1.455	0.888	0.064	14.134	−0.080
8	35.26	1.447	0.917	0.060	13.843	−0.078	1.390	0.871	0.076	14.177	−0.089
10	35.07	1.398	0.964	0.051	14.064	−0.068	1.322	0.917	0.065	14.340	−0.078
15	34.98	1.384	1.044	0.043	14.318	−0.062	1.276	0.981	0.060	14.542	−0.074

Table 11. Equivalent atomic number (Z_{eq}) and GP exposure (EBF) and energy absorption (EABF) buildup factor coefficients for $40ZnO–60TeO_2$ glass sample.

		EBF					EABF				
Energy (MeV)	Z_{eq}	b	c	a	X_k	d	b	c	a	X_k	d
0.015	25.70	1.004	1.518	−0.528	5.664	0.342	1.004	1.517	−0.528	5.784	0.342
0.02	25.82	1.012	0.138	0.608	11.377	−0.602	1.010	0.261	0.317	18.038	−0.292
0.03	26.03	1.020	0.374	0.190	29.160	−0.314	1.027	0.319	0.252	18.801	−0.191
0.04	39.66	3.492	0.323	0.111	21.988	−0.042	1.691	0.436	0.091	21.511	−0.043
0.05	40.11	2.856	0.077	−0.248	12.075	0.031	1.535	0.189	−0.137	8.704	0.104
0.06	40.44	2.275	0.041	1.015	17.114	−0.147	1.306	0.055	0.743	14.225	−0.187
0.08	40.85	1.626	0.064	0.724	14.368	−0.245	1.296	0.104	0.546	14.066	−0.220
0.1	41.13	1.165	0.312	0.283	13.758	−0.152	1.205	0.269	0.317	14.109	−0.164
0.15	41.55	1.249	0.495	0.172	14.407	−0.089	1.467	0.325	0.278	14.083	−0.159
0.2	41.79	1.477	0.518	0.171	14.281	−0.098	2.284	0.312	0.315	14.022	−0.197
0.3	42.08	1.587	0.732	0.080	14.487	−0.043	2.381	0.558	0.159	14.057	−0.098
0.4	42.24	1.705	0.888	0.039	14.179	−0.034	2.664	0.710	0.108	13.909	−0.087
0.5	42.34	1.766	0.973	0.017	14.318	−0.024	2.681	0.824	0.069	13.899	−0.065
0.6	42.40	1.788	1.019	0.005	13.944	−0.019	2.638	0.886	0.049	13.758	−0.054
0.8	42.47	1.796	1.068	−0.007	14.024	−0.013	2.494	0.960	0.027	13.658	−0.041
1	42.49	1.777	1.088	−0.012	13.430	−0.011	2.362	0.995	0.016	13.547	−0.032
1.5	41.41	1.628	1.162	−0.030	7.557	0.001	1.941	1.095	−0.012	13.269	−0.014
2	38.94	1.620	1.126	−0.021	11.860	−0.005	1.847	1.061	−0.002	12.338	−0.020
3	36.42	1.580	1.063	−0.002	12.597	−0.023	1.702	0.989	0.021	12.848	−0.042
4	35.53	1.524	1.023	0.013	13.161	−0.035	1.574	0.956	0.034	13.773	−0.054
5	35.08	1.500	0.974	0.031	13.429	−0.051	1.512	0.911	0.136	13.960	−0.071
6	34.78	1.462	0.959	0.039	13.519	−0.058	1.446	0.899	0.059	14.153	−0.076
8	34.44	1.436	0.922	0.058	13.802	−0.075	1.378	0.881	0.071	14.161	−0.084
10	34.26	1.385	0.963	0.050	14.045	−0.067	1.310	0.922	0.062	14.339	−0.075
15	34.17	1.360	1.035	0.044	14.338	−0.062	1.259	0.977	0.060	14.575	−0.073

substitution of TeO_2 by ZnO, while molar volume decreases from 30.067 to 24.766 (cm^3 mol^{-1}). The increase in density indicates that the zinc ions enter the tellurite glass network, which is related to the variation of the molar volume of the samples. The decrease in the molar volume is due to the decrease in the bond length or inter-atomic spacing between the atoms, which may be attributed to the increase in the stretching force constants (216 – 217.5 N m^{-1}) of the bonds inside the glass network. Hence the radius of Zn^{2+} (0.074 nm) is much smaller than that of Te^{2+} (0.097 nm), resulting in a more compact and dense glass. The addition of ZnO probably causes a change in crosslink density and coordination number of Te^{2+} ions [31].

4.1 *Mass attenuation coefficient (μ_m)*

Experimental and theoretical values of mass attenuation coefficients for seven glass samples at gamma energies 0.662, 1.173 and 1.33 MeV have been given in table 2. The theoretical values of mass attenuation coefficients were calculated from WinXCom [28]. Estimated error in the experimental measurements was $\leq$2%. It is clear from table 2 that the mass attenuation coefficients of glass samples decrease with increasing gamma energies. At low photon energy the prominent reaction between the studied glass samples barriers and gamma rays is the photoelectric effect, which decreases with increasing gamma energy. The behaviour of the mass attenuation coefficient at intermediate photon energy may be attributed to the Compton scattering process. The values of the mass attenuation coefficient are dependent on the elemental composition and consequently on the glass density [32]. Experimental results of μ_m increase with increasing ZnO content. This behaviour may be attributed to the fact that addition of ZnO increases the glass density and decreases the molar volume, which indicates that the glass structure becomes more compact and dense. The experimental mass attenuation coefficient values are in good agreement with the theoretical values.

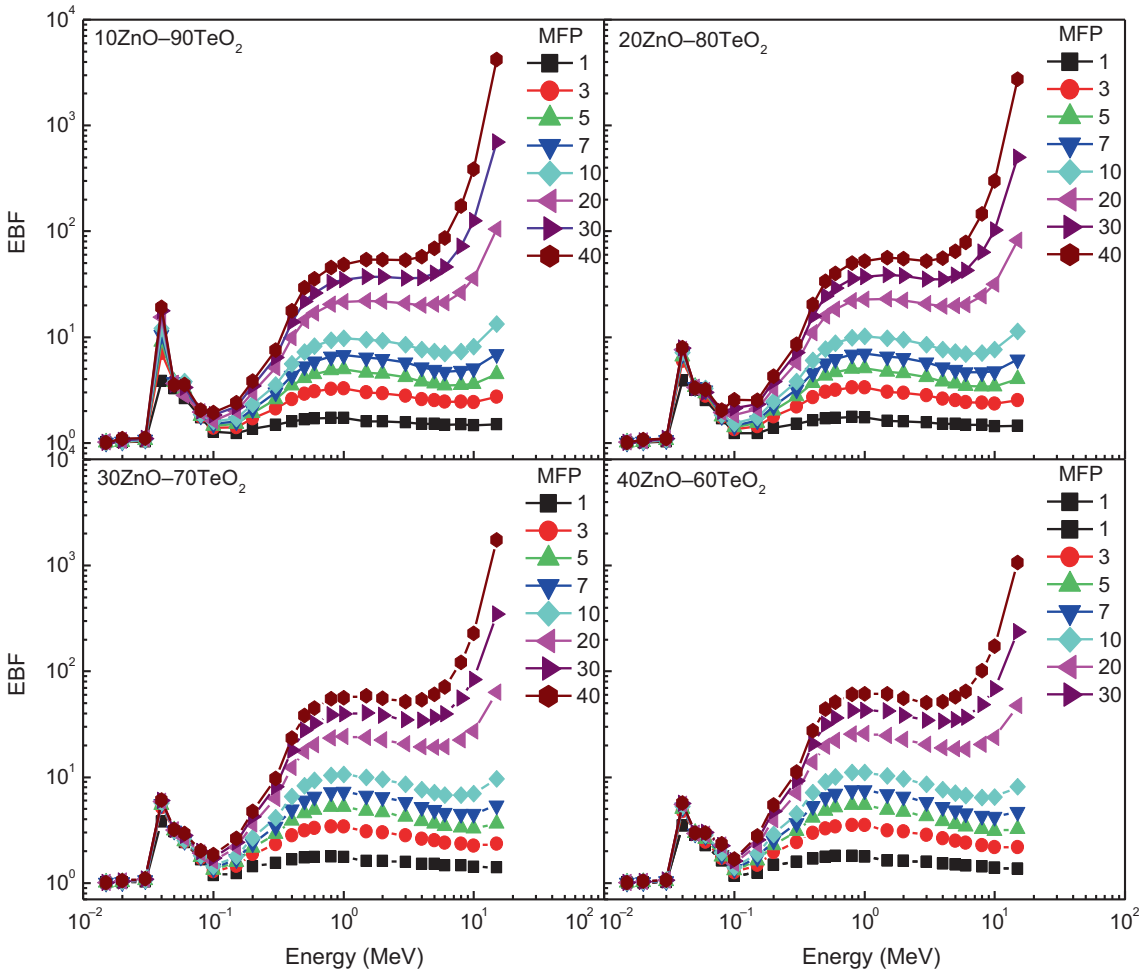

Figure 6. The exposure buildup factor (EBF) for the glass samples in the energy region 0.015–15 MeV at different penetration depths.

4.2 *HVL and MFP*

The HVL was calculated using linear attenuation coefficient (cm^{-1}) as follows:

$$\mathrm{HVL} = \frac{\ln(2)}{\mu}, \tag{12}$$

where μ is the linear attenuation coefficient. The values of HVL are listed in table 3. Figure 2 shows that the HVL values decrease with increasing ZnO in glass systems at photon energies 0.662, 1.173 and 1.33 MeV, which is due to increase in mass attenuation coefficient and density on replacing TeO_2 by ZnO. As shown in figure 2, the HVL of glass samples is lower than HVL of barite and ferrite concretes at 0.662 and 1.33 MeV photon energies [22]. It has been observed that the ZnO–TeO_2 class system is found to be better than concrete, indicating the potential of utilizing the prepared glasses as radiation shields.

The values of MFP (cm^{-1}) of the prepared glass samples have been obtained using the following equation:

$$\mathrm{MFP} = \frac{1}{\mu}. \tag{13}$$

Table 3 reports the values of MFP of prepared glass samples, which decrease with increasing ZnO content. The MFP values of ZnO–TeO_2 glasses were compared to those of some standard radiation shielding concretes (figure 3) [33]. Figure 3 shows that for the glass samples having 10 mol% of zinc oxide or higher, the values of MFP are lower than those of ilmenite, basalt-magnetite, hematite-serpentine and ordinary concretes at 0.662, 1.173 and 1.33 MeV photon energy. This means that the glass samples are better radiation shielding materials in comparison with standard shielding concretes. A material to be used as a gamma-ray radiation shielding material must have low values of HVL and MFP. Therefore, it is indicated that ZnO–TeO_2 glass systems, which show low values of HVL and

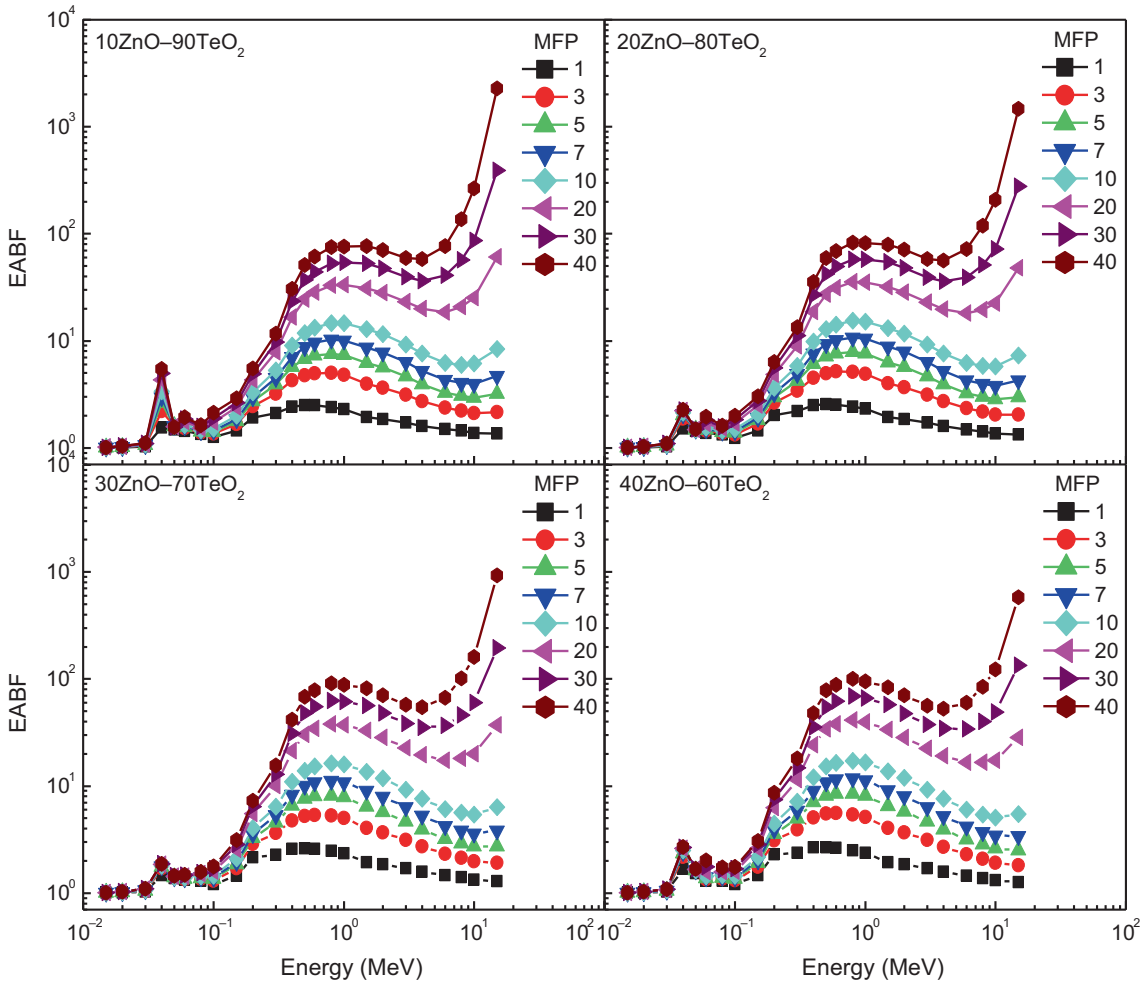

Figure 7. The energy absorption buildup factor (EABF) for the glass samples in the energy region 0.015–15 MeV at different penetration depths.

MFP at photon energy 0.662, 1.173 and 1.33 MeV, are good gamma-ray shielding glass systems. Hence, it is proposed that the prepared glass samples can be promising nominees as non-conventional alternate gamma-ray shielding materials.

4.3 *Effective atomic number (Z_{eff}) and electron density (N_{el})*

The effective atomic number (Z_{eff}) and electron density (N_{el}) for glass samples in the energy range 0.015–15 MeV are presented in table 4. Equations (5) and (6) have been used, respectively, to calculate the effective atomic number (Z_{eff}) and electron density (N_{el}). The variation of Z_{eff} with photon energy for total interaction processes in all glasses is shown in figure 4. It can be seen that initially photoelectric interaction dominates and effective atomic number remains almost constant in the energy range 0.015–0.03 MeV; then it starts increasing, reaches a maximum at 0.04 MeV and then it decreases sharply with increasing energy up to 1 MeV, which indicates that the Compton scattering process starts taking place. In the intermediate energy region (0.6–2 MeV), the Z_{eff} values are found to be almost constant for the selected materials, which clearly indicates that Compton scattering cross-section depends only on the energy and is almost independent of the composition of the materials. Finally, the effective atomic number increases with increasing photon energy. This is due to the pre-dominance of the pair production process, whose cross-section is proportional to Z^2. Figure 4 shows that even in the photon energy range 0.04–0.6 MeV the 10ZnO–TeO_2 glass sample has the highest effective atomic number. The variation of electron density for investigated glass systems with photon energy in the range 0.015–15 MeV demonstrates the same behaviour as that of Z_{eff}, as shown in figure 5.

4.4 *Gamma-ray buildup factors of the glass samples*

The calculated equivalent atomic numbers (Z_{eq}), EBF and EABF GP fitting parameters for glass samples in the energy region 0.015–15 MeV are shown in tables 5–11. Figures 6 and 7 show the variations of EBF and EABF with a photon energy of the given glass samples at different penetration depth, respectively. It is observed that EBF and EABF of glass samples are small at low and high (8 MeV) energies. This may be attributed to the absorption processes, photoelectric effect and pair production dominating the low and

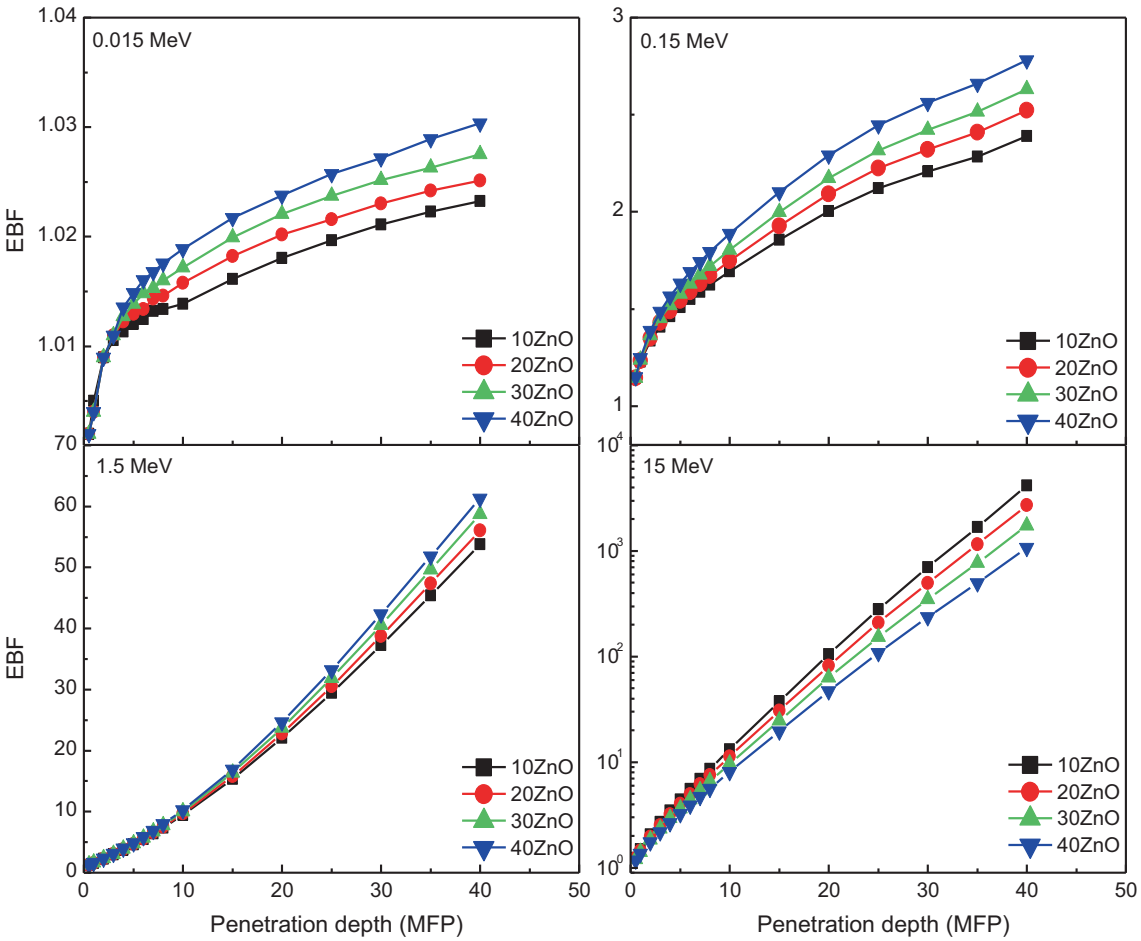

Figure 8. The exposure buildup factor for the glass samples up to 40 MFP at 0.015, 0.15, 1.5 and 15 MeV.

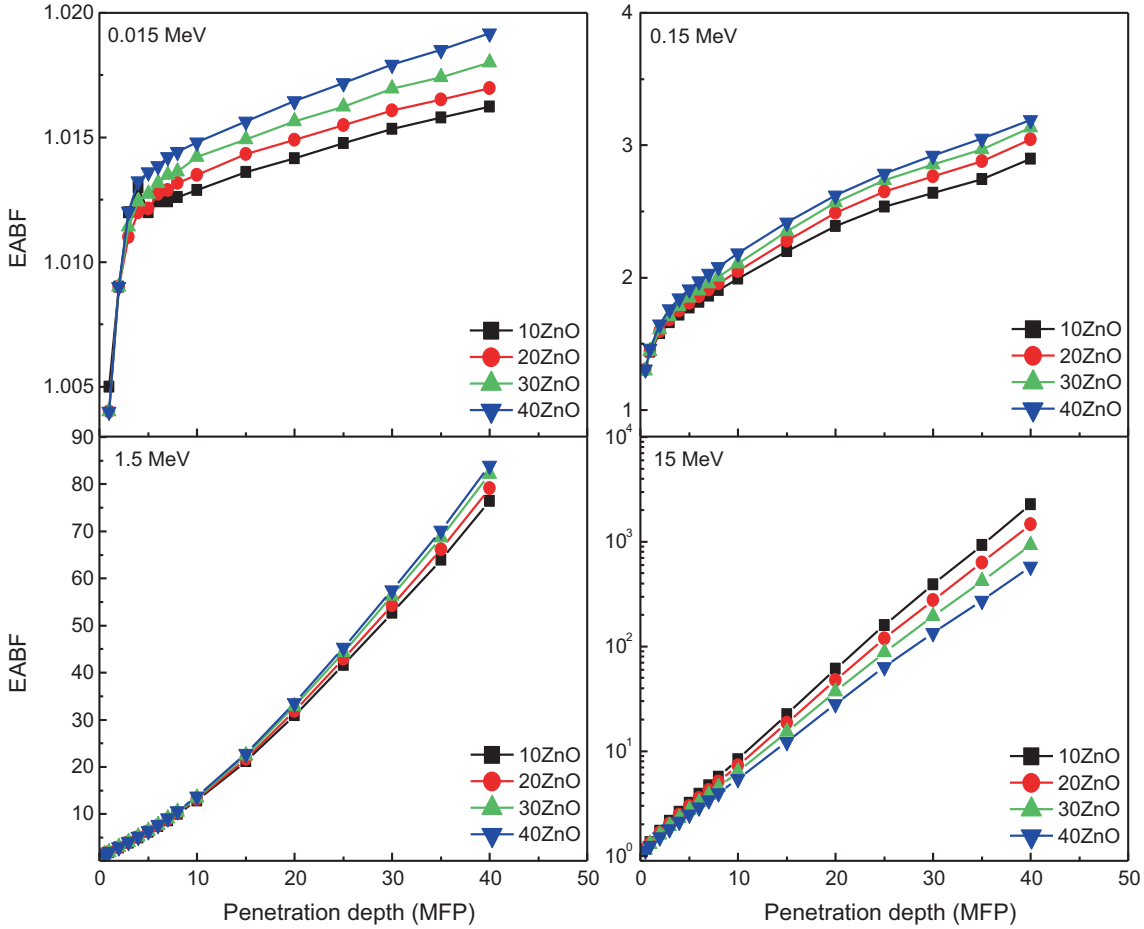

Figure 9. The energy absorption buildup factor for the glass samples up to 40 MFP at 0.015, 0.15, 1.5 and 15 MeV.

high energy regions, respectively, in which photons are completely absorbed or removed. A sharp peak in the EBF and EABF values was observed at 40 keV energy, as shown in figures 6 and 7, which may be due to the K-absorption edge of Te at around 31.8 keV. Around the K-edge of high-Z elements, mass attenuation coefficients jump to a huge value on the upper side of the K-edge and the element has two mass attenuation coefficients corresponding to the lower and upper side of the edge. This abrupt change in mass attenuation coefficient could lead to a sharp peak in buildup factor. Then the EBF and EABF values increase with the increase in photon energy and show a maximum at 0.8 MeV due to multiple scattering by Compton scattering at the intermediate energies. In Compton scattering, photons are not completely removed, but degraded in energy. Finally, BF values start decreasing with the further increase in photon energy up to 8 MeV due to pair production. We found that EBF and EABF values increased at high energy (>8 MeV) for all the glass samples with increasing penetration depths, which might be due to the increase in multiple scattering as the penetration depth increases. The dependence on the chemical composition was the same as that observed elsewhere [34,35].

Figures 8 and 9 show the variations of EBF and EABF with penetration depth at incident photon energies 0.015, 0.15, 1.5 and 15 MeV. It is clear that the EBF and EABF values increase with increasing penetration depths for glass samples. At a low penetration depth up to 3 MFP and 0.15 MeV incident photon energy, the EBF and EABF values remain constant with increasing ZnO content. At the photon energy of 1.5 MeV, the EBF and EABF values remain constant with increasing ZnO content and penetration depth up to 20 MFP. This may be due to domination of photoelectric absorption, which depends on Z_{eq}^{4-5} at photon energy below 0.15 MeV. In the high photon energy region (>2 MeV) another absorption process, pair/triplet production, takes over the Compton scattering process.

5. Conclusions

Mass attenuation coefficient (μ_{m}), HVL and MFP for $x\mathrm{ZnO}-(100-x)\mathrm{TeO_2}$, where $x = 10$, 15, 20, 25, 30, 35 and 40 mol%, have been measured for 0.662, 1.173 and 1.33 MeV

photons emitted from ^{137}Cs and ^{60}Co using a 3 × 3 inch NaI(Tl) detector. The experimental mass attenuation coefficients were found to decrease with increasing gamma energy and increase with increasing ZnO concentration. HVL and MFP at selected photon energies increase with increasing gamma energy and decrease with increasing ZnO concentration. Results show that for the glass samples having 10 mol% of zinc oxide or higher, the values of MFP are lower than those of ilmenite, basalt-magnetite, hematite-serpentine and ordinary concretes at 0.662, 1.173 and 1.33 MeV photon energy. Effective atomic numbers (Z_{eff}) and electron densities (N_{el}) of glass samples have been calculated in the photon energy range 0.015–15 MeV and they have been found to be clearly energy dependent. The GP fitting method has been used for calculation of EBF and EABF of given glass samples in the energy range 0.015–15 MeV up to 40 penetration depths. The 10ZnO–90TeO_2 glass sample was found to have lower values of gamma-ray EBFs in the intermediate energy region. The EBF and EABF were found to be energy- and penetration-depth-dependent parameters as well.

References

[1] Kulwinder K, Singh J and Vikas A 2015 *Nucl. Eng. Des.* **285** 31
[2] Aly S, Elshazly M, Elbashar H, AbouEl-azm M, El-Okr M, Comsan H *et al* 2014 *Radiat. Phys. Chem.* **102** 167
[3] Singh J, Sandeep K and Kaundal S 2014 *Radiat. Phys. Chem.* **96** 153
[4] Vishwanath S, Badiger N, Chanthima N and Kaewkhao J 2014 *Radiat. Phys. Chem.* **98** 14
[5] Wang J S, Vogel E M and Snitzer E 1994 *Opt. Mater.* **3** 187
[6] Ulrich D R 1964 *J. Am. Ceram. Soc.* **47** 595
[7] Burger H, Kneipp K, Hobert H, Vogel W, Kozhukharov V and Neov S 1992 *J. Non-Cryst. Solids* **151** 134
[8] Senthil Murugan G, Suzuki T, Ohishi Y, Takahashi Y, Benino Y, Fujiwara T *et al* 2004 *Appl. Phys. Lett.* **85** 3405
[9] Manikandan N, Ryasnyanskiy A and Toulouse J 2012 *J. Non-Cryst. Solids* **358** 947
[10] Sekiya T, Mochida N and Ohtsuka A 1994 *J. Non-Cryst. Solids* **168** 106
[11] Sekiya T, Mochida N and Ohtsuka A 1992 *J. Non-Cryst. Solids* **144** 128
[12] Sharaf J M and Saleh H 2015 *Radiat. Phys. Chem.* **110** 87
[13] Salehi D, Sardari D and Jozani M S 2015 *Adv. Mater. Res.* **4** 23
[14] Harima Y, Sakamoto Y, Tonaka S and Kawai M 1986 *Nucl. Sci. Eng.* **94** 24
[15] Suteau C and Chiron M 2005 *Radiat. Prot. Dosim.* **116** 489
[16] Shimizu A 2002 *J. Nucl. Sci. Technol.* **39** 477
[17] Shimizu A, Onda T and Sakamoto Y 2004 *J. Nucl. Sci. Technol.* **41** 413
[18] Sandari D, Abbaspour A, Baradaran S and Babapour F 2009 *Appl. Radiat. Isot.* **67** 1438
[19] ANSI/ANS-6.4.3 1991 *Gamma ray attenuation coefficient and buildup factors for engineering materials*
[20] Singh V P, Badiger N M and Kaewkhao J 2014 *J. Non-Cryst. Solids* **404** 167
[21] Chanthima N and Kaewkhao J 2013 *Ann. Nucl. Eng.* **55** 23
[22] Singh K, Kaur S and Kaundal R 2014 *Radiat. Phys. Chem.* **96** 153
[23] Ruengsri S, Insiripong S, Sangwaranatee N and Kaewkhao J 2015 *Prog. Nucl. Eng.* **83** 99
[24] Singh V P, Badiger N M, Chanthima N and Kaewkhao J 2014 *Radiat. Phys. Chem.* **98** 14
[25] Kurudirek M 2014 *Nucl. Eng. Des.* **280** 440
[26] Burger H and Vogel W 1985 *Infrared Phys.* **25** 395
[27] Sidek H, Chow S, Talib Z and Halim S 2004 *Turk. J. Phys.* **28** 65
[28] Sidek H, Rosmawati S, Talib Z, Halimah M K and Daud W 2009 *Am. J. Appl. Sci.* **6** 1489
[29] Gerward L, Guilbert N, Jensen K B and Levring H 2001 *Radiat. Phys. Chem.* **60** 23
[30] Gerward L, Guilbert N, Jensen K B and Levring H 2004 *Radiat. Phys. Chem.* **71** 653
[31] Harima Y 1983 *Nucl. Sci. Eng.* **83** 299
[32] Harima Y 1993 *Radiat. Phys. Chem.* **41** 631
[33] Bootjomchai C, Laopaiboon J, Yenchai C and Laopaiboon R 2012 *Radiat. Phys. Chem.* **81** 785
[34] Kurudirek M and Özdemir Y 2011 *J. Radiol. Prot.* **31** 117
[35] Esra K, Ufuk P, Neslihan E and Yüuksel Ö 2016 *Int. J. Radiat. Biol.* **28** 1